THE JOURNAL OF BIOLOGICAL CHEMISTRY VOL. 289, NO. 9, pp. 6028–6040, February 28, 2014

Phosphatidylinositol 4,5-Biphosphate (PIP_2) Modulates Interaction of Syntaxin-1A with Sulfonylurea Receptor 1 to Regulate Pancreatic β-Cell ATP-sensitive Potassium Channels*

Received for publication, August 19, 2013, and in revised form, January 12, 2014 Published, JBC Papers in Press, January 15, 2014, DOI 10.1074/jbc.M113.511808

Tao Liang[‡1], Li Xie[‡1,2], Christin Chao[‡§1], Youhou Kang[‡], Xianguang Lin[‡], Tairan Qin[‡], Huanli Xie[‡], Zhong-Ping Feng[§], and Herbert Y. Gaisano[‡§3]

From the Departments of [‡]Medicine and [§]Physiology, University of Toronto, Toronto, Ontario M5S 1A8, Canada

Background: PIP_2 actions on activating K_{ATP} channels are not only on Kir6.2 but may be also on syntaxin-1A, to modulate syntaxin-1A actions on SUR1.
Results: PIP_2 disrupts Syn-1A·SUR1 interactions by reducing syntaxin-1A availability to inhibit of K_{ATP} channels.
Conclusion: PIP_2 modulates syntaxin-1A·SUR interactions.
Significance: Membrane phospholipid composition in health and diabetes profoundly affect β-cell K_{ATP} channels by several mechanisms to influence insulin secretion.

In β-cells, syntaxin (Syn)-1A interacts with SUR1 to inhibit ATP-sensitive potassium channels (K_{ATP} channels). PIP_2 binds the Kir6.2 subunit to open K_{ATP} channels. PIP_2 also modifies Syn-1A clustering in plasma membrane (PM) that may alter Syn-1A actions on PM proteins like SUR1. Here, we assessed whether the actions of PIP_2 on activating K_{ATP} channels is contributed by sequestering Syn-1A from binding SUR1. *In vitro* binding showed that PIP_2 dose-dependently disrupted Syn-1A·SUR1 complexes, corroborated by an *in vivo* Forster resonance energy transfer assay showing disruption of SUR1-(-EGFP)/Syn-1A(-mCherry) interaction along with increased Syn-1A cluster formation. Electrophysiological studies of rat β-cells, INS-1, and SUR1/Kir6.2-expressing HEK293 cells showed that PIP_2 dose-dependent activation of K_{ATP} currents was uniformly reduced by Syn-1A. To unequivocally distinguish between PIP_2 actions on Syn-1A and Kir6.2, we employed several strategies. First, we showed that PIP_2-insensitive Syn-1A-5RK/A mutant complex with SUR1 could not be disrupted by PIP_2, consequently reducing PIP_2 activation of K_{ATP} channels. Next, Syn-1A·SUR1 complex modulation of K_{ATP} channels could be observed at a physiologically low PIP_2 concentration that did not disrupt the Syn-1A·SUR1 complex, compared with higher PIP_2 concentrations acting directly on Kir6.2. These effects were specific to PIP_2 and not observed with physiologic concentrations of other phospholipids. Finally, depleting endogenous PIP_2 with polyphosphoinositide phosphatase synaptojanin-1, known to disperse Syn-1A clusters, freed Syn-1A from Syn-1A clusters to bind SUR1, causing inhibition of K_{ATP} channels that could no longer be further inhibited by exogenous Syn-1A. These results taken together indicate that PIP_2 affects islet β-cell K_{ATP} channels not only by its actions on Kir6.2 but also by sequestering Syn-1A to modulate Syn-1A availability and its interactions with SUR1 on PM.

Pancreatic β-cell regulates glucose-stimulated insulin secretion through association with ATP-sensitive potassium channels (K_{ATP} channels).[4] The K_{ATP} channel is a hetero-octamer with four Kir6.2 (inward rectifier K^+ 6.2) subunits forming a conduction channel surrounded by four regulatory SUR1 subunits (1). β-Cell plasma membrane (PM) excitability and insulin secretion are set by concentration of nucleotides, ATP, and ADP (2, 3). The physiologic β-cell secretagogue is glucose, which, upon entry and metabolism in β-cells, increases ATP production, causing K_{ATP} channel closure leading to cellular depolarization (4), which activates L-type voltage-dependent Ca^{2+} channels, with resulting Ca^{2+} influx triggering exocytotic fusion of insulin granules with PM (4, 5). Conversely, when plasma glucose levels fall, increase in ADP and decrease in ATP concentrations lead to K_{ATP} channel activation, with ensuing PM hyperpolarization, which reduces insulin release.

In addition to adenine nucleotides, K_{ATP} channels are regulated by other endogenous factors in β-cells, particularly phosphatidylinositol 4,5-biphosphate (PIP_2). PIP_2, comprising only 1% of PM phospholipids, stimulates activity of ATP-sensitive and -insensitive Kir channels by increasing channel open probability (6). PIP_2 is an indispensable membrane phosphoinositide that participates in a wide variety of other cellular func-

* This work was supported by Canadian Institutes of Health Research Grant MOP 69083 (to H. Y. G.) and by an equipment grant to the 3D (Diet, Digestive Tract, and Disease) Centre from the Canadian Foundation for Innovation and Ontario Research Fund (Project 19442).
[1] These authors contributed equally to this work.
[2] Supported by a fellowship from the Canadian Diabetes Association.
[3] To whom correspondence should be addressed: University of Toronto, 1 Kings College Circle, Rm. 7368, Toronto M5S 1A8, Ontario Canada. Tel.: 416-978-1526; Fax: 416-978-8765; E-mail: herbert.gaisano@utoronto.ca.

[4] The abbreviations used are: K_{ATP} channel, ATP-sensitive potassium channel; PM, plasma membrane; PIP_2 or $PI(4,5)P_2$, phosphatidylinositol 4,5-biphosphate; IP_3, inositol 1,4,5-trisphosphate; $PI(3,5)_2$, phosphatidylinositol 3,5-biphosphate; PIP_3, inositol 1,4,5-trisphosphate; SUR1, sulfonylurea receptor 1; Syn-1A, syntaxin-1A; TIRFM, total internal reflection fluorescence microscopy; EGFP, enhanced green fluorescent protein; pF, picofarads; aa, amino acids; NBF, nucleotide-binding fold.

tions, including production of second messengers, endo- and exocytosis, and regulation of ion channels, transporters, and actin cytoskeleton (7–11). For K_{ATP} channel regulation, a negatively charged inositol triphosphate headgroup of PIP_2 interacts electrostatically with positively charged amino acid residues in N- and C-terminal cytoplasmic domains of Kir6.2 (12, 13). However, several studies demonstrated that the SUR subunit plays an essential role in stabilizing PIP_2-Kir6.2 interaction. For instance, a brief application of PIP_2 shifted ATP inhibition of Kir6.1/SUR1 channels compared with Kir6.2 alone, and this PIP_2 recovery was more stable when SUR1 was present, thus indicating that SUR increases PIP_2 binding and stimulation on Kir6.2 (14, 15). A recent report showed that a mutation in SUR1-TMD0 induces spontaneous Kir6.2 current decay and was reversed with exogenous PIP_2 (16). PIP_2 therefore plays versatile roles in controlling β-cell K_{ATP} channel activities and insulin exocytosis (12, 17). Lin *et al.* (18) showed that disrupting K_{ATP} channel and PIP_2 interaction by overexpressing PIP_2-insensitive Kir6.2 mutants caused cellular depolarization and elevated basal insulin secretion. Conversely, up-regulation of PIP_2 expression causing activation of K_{ATP} channels resulted in cellular hyperpolarization, which reduced insulin secretion despite the presence of high glucose (18).

Besides the aforementioned actions of PIP_2 on various ion channels, PIP_2 also interacts with various components of the exocytotic fusion machinery, including CAPS, synaptotagmins, rabphilin, and Syn-1A (19–23). Syn-1A is one of three SNARE (soluble *N*-ethylmaleimide-sensitive factor attachment protein receptor) proteins that form the ternary complex constituting the minimal membrane fusion machinery in neurons and neuroendocrine cells (24). Besides its role in membrane fusion machinery, Syn-1A appears to play additional roles in the secretory process, effectively regulating various calcium and potassium channels involved in both initiating and terminating exocytosis (25).

In a body of work, we have shown that Syn-1A could act as an endogenous regulator exhibiting potent inhibitory action on β-cell K_{ATP} channels (25–28). We identified specific conserved motifs within the nucleotide binding domains of SUR1 that functionally interact with Syn-1A (28). Syn-1A contains highly charged, polybasic juxtamembrane motif in which neutralizing mutations abrogated Syn-1A-PIP_2 electrostatic interaction, causing a reduction in exocytosis by influencing the clustering of Syn-1A molecules on PM required for efficient membrane fusion (21, 22). In this study, we investigated the hypothesis that these actions of PIP_2 on Syn-1A could influence Syn-1A interactions with SUR1 to affect K_{ATP} channel activities in β-cells.

EXPERIMENTAL PROCEDURES

Material—Syn-1A mutant in which highly conserved polybasic juxtamembrane residues (within the cytoplasmic domain) between positions 260 and 265 (Lys-260, -264, and -265; Arg-262 and -263) constituting the major lipid-binding domain were mutated to alanine, called the Syn-1A-5RK/A mutant (gift from Ed Stuenkel, University of Michigan, Ann Arbor, MI), which abrogates Syn-1A binding to PIP_2 (29). A polyphosphoinositide 5-phosphatase synaptojanin 1 (HA-IPP1-CAAX tagged with RFP) construct in pcDNA3 (a gift from Geert van den Bogaart and Reinhard Jahn, Max-Planck Institute for Biophysical Chemistry, Gottingen, Germany) was used to deplete endogenous $PI(4,5)P_2$ from the PM (30, 31).

Pancreatic Islet β-Cell Isolation—Single male Wistar rat pancreatic β-cells were enzymatically dispersed from isolated islets as described (32), plated on coverslips, and cultured in RPMI 1640 (supplemented with 2.8 mM glucose, 7.5% FCS, 0.25% sodium, 100 μg/ml streptomycin) prior to recordings.

HEK293 Cell Transfection—To examine the differences between Syn-1A-WT and Syn-1A-5RK/A, HEK293 cells were co-transfected with rat Kir6.2 (gift from S. Seino, Chiba University, Chiba, Japan) and SUR1-EGFP (gift from C. G. Nichols, Washington University, St. Louis, MO) and then trypsinized and plated on glass coverslips for 17–18 h prior to electrophysiological experiments. For FRET imaging recording, HEK293 cells were co-transfected with full-length Syn-1A (aa 1–288)-mCherry or full-length Syn-1A-5RK/A-mCherry (acceptor) and SUR1-EGFP (donor) as reported (33), along with Kir6.2, using Lipofectamine 2000 (Invitrogen). FRET imaging was conducted 2 days after transfection.

In Vitro Binding Assay and Western Blotting—*In vitro* binding assays were performed as described (34). Briefly, 250 pmol of GST (control) and GST-Syn-1A (aa 1–265) or GST-Syn-1A-5RK/A (aa 1–265), both containing only the cytoplasmic domain bound to glutathione-agarose beads, were incubated with lysate extract of HEK293 cells (400 μg of protein) co-transfected with SUR1 and Kir6.2 in lysis buffer in the presence of increasing concentrations of PIP_2 or other indicated phospholipids (Echelon Biosciences Inc.) at 4 °C for 2 h with constant agitation. Beads were washed three times, and samples were separated on 10% SDS-PAGE, transferred to nitrocellulose membrane, and identified with anti-SUR1 antibody (1:1,000; gift from J. Ferrer, Barcelona, Spain).

Electrophysiology—K_{ATP} channel recordings were performed on INS-1E cells using the inside-out patch clamp technique (35) and on rat β-cells and HEK293 cells using the whole-cell patch-clamp technique. Pipette resistance when filled with solution was 1.0–1.5 megaohms. GST, GST-Syn-1A, ATP (Sigma-Aldrich) and PIP_2 (Sigma-Aldrich) were perfused onto the cytoplasmic side of excised membrane patches. Membrane patches were held at −50 mV to evoke inward currents. For β-cell, HEK293, and INS-1 cell voltage-clamped whole-cell studies, membrane potential was held at −70 mV, and a pulse of −140 mV (500 ms) was given every 10 s to monitor K_{ATP} current magnitude. Pipette resistance was 2–4 megaohms. Bath solution contained 140 mM NaCl, 4 mM KCl, 1 mM $MgCl_2$, 2 mM $CaCl_2$, 10 mM HEPES, 2 mM glucose, pH 7.3. Pipette solution contained 140 mM KCl, 1 mM $MgCl_2$, 1 mM EGTA, 10 mM HEPES, pH 7.25. GST, GST-Syn-1A, and PIP_2 were added to intracellular solution for dialysis into cells via patch pipette. Tolbultamide (0.1 mM; Tolb) was perfused into bath solution after maximum current reached to completely inhibit and verify the K_{ATP} current. All recordings were carried out at 22–24 °C using an EPC10 amplifier with Pulse version 8.77 acquisition software (HEKA Electronik, Lambrecht, Germany). Data were sampled at 1 kHz.

FRET Imaging—As described previously (33), FRET study by total internal reflection fluorescence microscopy (TIRFM)

assesses molecular interactions on the surface of PM, avoiding contamination from intracellular FRET signals. HEK293 cells were transfected with different combinations of plasmids 2 days prior to the experiment, where EGFP fused with SUR1 was used as the FRET donor, and mCherry fused with full-length Syn-1A or full-length Syn-1A-5RK/A was used as the FRET acceptor; Kir6.2 co-infected to express functional K_{ATP} channels localized correctly on PM. For FRET analysis, four images, including donor excitation/donor emission (*Dd*), donor excitation/acceptor emission (*Da*), acceptor excitation/acceptor emission (*Aa*), and acceptor excitation/donor emission (*Ad*), were acquired under same conditions. Donor-only and acceptor-only samples were acquired at the beginning of each experiment for bleed-through calculation. FRET efficiency was used to indicate interaction of the two proteins, calculated with the equation, FRET efficiency % = $(((FRET_{raw} - (CoB \times Dd_{FRET}) - (CoA \times Aa_{FRET}))/Dd_{FRET}) \times 100\%$, where *CoB* is the amount of donor bleed-through in the absence of acceptor, and *CoA* is the amount of acceptor bleed-through in the absence of donor.

After baseline FRET images were taken, the cells were permeabilized with digitonin (10 μg/ml in intracellular buffer, 5 min, 37 °C). FRET images were then taken again, followed by perfusion with the indicated lipids for another 5 min, and then we waited for another 7–10 min before the final FRET images were captured. Intracellular buffer contained 20 mM HEPES, 5 mM NaCl, 140 mM potassium gluconate, and $MgCl_2$, pre-equilibrated with O_2/CO_2 = 95:5, pH 7.4, at 37 °C. PIP_2, powder dissolved in double-distilled H_2O, was sonicated for 30–45 s to a stock concentration of 920 mM (per the manufacturer's instructions). This PIP_2 stock was diluted to the indicated concentrations in intracellular buffer and sonicated again for 30 s before adding to the cells.

Statistical Analysis—For statistical analysis of FRET efficiency, regions of interest were drawn around entire areas of the PM surface expressing any FRET signal (*blue*, *green*, or *red*; see the *pseudocolor bar* in Figs. 5, 7, and 9) as indicated, not including the *purple* areas having no FRET signal. From these regions of interest, FRET efficiency was calculated as mean ± S.E., and values were compared using the Mann-Whitney test by SigmaStat version 3.1 (Systat Software Inc., Chicago, IL). For electrophysiological experiments, data analysis was done using SigmaPlot version 11.0 (Systat Software Inc.). Data obtained from concentration-response curves were fitted to the drug responsiveness equation, $Y = ((A1 - A2)/(1 + (X + X0)p)) + A2$. Where *Y* is K_{ATP} current at different [PIP_2], *A1* is K_{ATP} current before PIP_2 application, *A2* is maximal K_{ATP} current activated by PIP_2, *X* denotes [PIP_2] applied to membrane patches, *X0* denotes [PIP_2] that produced half-maximal K_{ATP} channel activation, and *p* is slope of the curve. Curve fitting was performed by Origin version 6.0. Inside-out electrophysiological data were analyzed using each cell as its own control. Whole-cell electrophysiological data are presented as mean ± S.E., expressed as current normalized to cell capacitance (pA/pF). For multiple groups, channel activity was compared using one-way analysis of variance, followed by the Student-Newman-Keuls post hoc test. For the binding assay and Western blotting, blots were quantified by densitometry scanning followed by analysis with Scion Image (beta-4.0.2, Scion Corp.). Data were compared using Student's *t* test. We considered $p < 0.05$ as a significant difference.

RESULTS

PIP_2 Dose-dependently Inhibits Syntaxin-1A Binding to SUR1—A Substantial body of evidence indicates that highly negatively charged membrane phosphatidylinositol polyphosphates interact with positively charged residues on the N and C termini of the cytoplastic domains of Kir channels (14, 35, 36). In addition, it is well established that highly charged, polybasic juxtamembrane regions of Syn-1A interact with PIP_2 (29); thus, the SNARE fusion machinery itself may be a target of regulation by phosphoinositides (22, 29, 37). Although there is strong evidence for the role of PIP_2 on Kir6.2 and SNARE protein interactions, we here explored the possibility that PIP_2 could activate K_{ATP} channels in a manner contributed by its actions on Syn-1A, which, in turn, perturbs Syn-1A binding to SUR1.

We examined whether increasing PIP_2 concentrations can disrupt Syn-1A binding to SUR1 by employing *in vitro* binding assays. GST-Syn-1A-bound glutathione-agarose beads were used to pull down SUR1 from lysate extracts of HEK293 cells co-infected with SUR1 and Kir6.2. After adding increasing PIP_2 concentrations (Fig. 1*A*), SUR1 binding to GST-Syn-1A did not decrease at 0.5 μM but was reduced by 41% at a physiologic concentration of 10 μM (38) and by 65% at 20 μM ($n = 3$; Fig. 1*A*). GST, as negative control, did not pull down SUR1. Importantly, GST-Syn-1A contains the cytoplasmic domain (aa 1–265) and no transmembrane domain (aa 266–288), and the PIP_2-binding domain is located at aa 260–265 (29). This indicates that PIP_2 binding of this Syn-1A cytoplasmic domain is sufficient to sequester Syn-1A and disrupt Syn-1A·SUR1 interactions. To demonstrate that these effects are selective to PIP_2 ($PI(4,5)P_2$ (38), we further assessed the effects of $PI(3,5)P_2$ (Fig. 1*B*), which has a negative charge similar to $PI(4,5)P_2$ and PIP_3 (*PI(3,4,5)P$_3$*; Fig. 1*C*), which has a stronger negative charge. At a physiologic concentration of 10 μM, the other phospholipids had little ($PI(3,5)P_2$; reduced by 17%, not significant) or no effect (PIP_3) on Syn-1A·SUR1 binding. At the highest concentration of 20 μM, these phospholipids disrupted Syn-1A·SUR1 binding but to a much lesser extent than $PI(4,5)P_2$ (at 65% reduction), for $PI(3,5)P_2$ (at 51% reduction) or PIP_3 (at 44% reduction). Importantly, PIP_2 is abundant in mammalian cells, whereas the other phospholipids are minor and not likely to reach these high concentrations (38). We then proceeded to dissect the functional implications PIP_2 disruption of Syn-1A·SUR1 interactions.

PIP_2 Activation of Kir6.2/SUR1 Channels Is Reduced by Syn-1A—We examined PIP_2 dose-response activation of the K_{ATP} channel on INS-1E cells in the absence and presence of 1 μM GST-Syn-1A using an inside-out patch clamp technique. Membrane patches were held at −50 mV to induce inward currents. Fig. 2, *A* and *B*, shows representative traces of the protocol utilized for PIP_2 in the absence and presence of Syn-1A. Membrane patches were initially exposed to 0, 1, and 3 mM ATP K_{int} solution to characterize K_{ATP} channels and verify the ATP sensitivity of recorded currents. In Fig. 2*A*, after patch excision, channels rapidly run down in the absence of ATP; however, subsequent exposure to 5, 10, and 20 μM PIP_2 gradu-

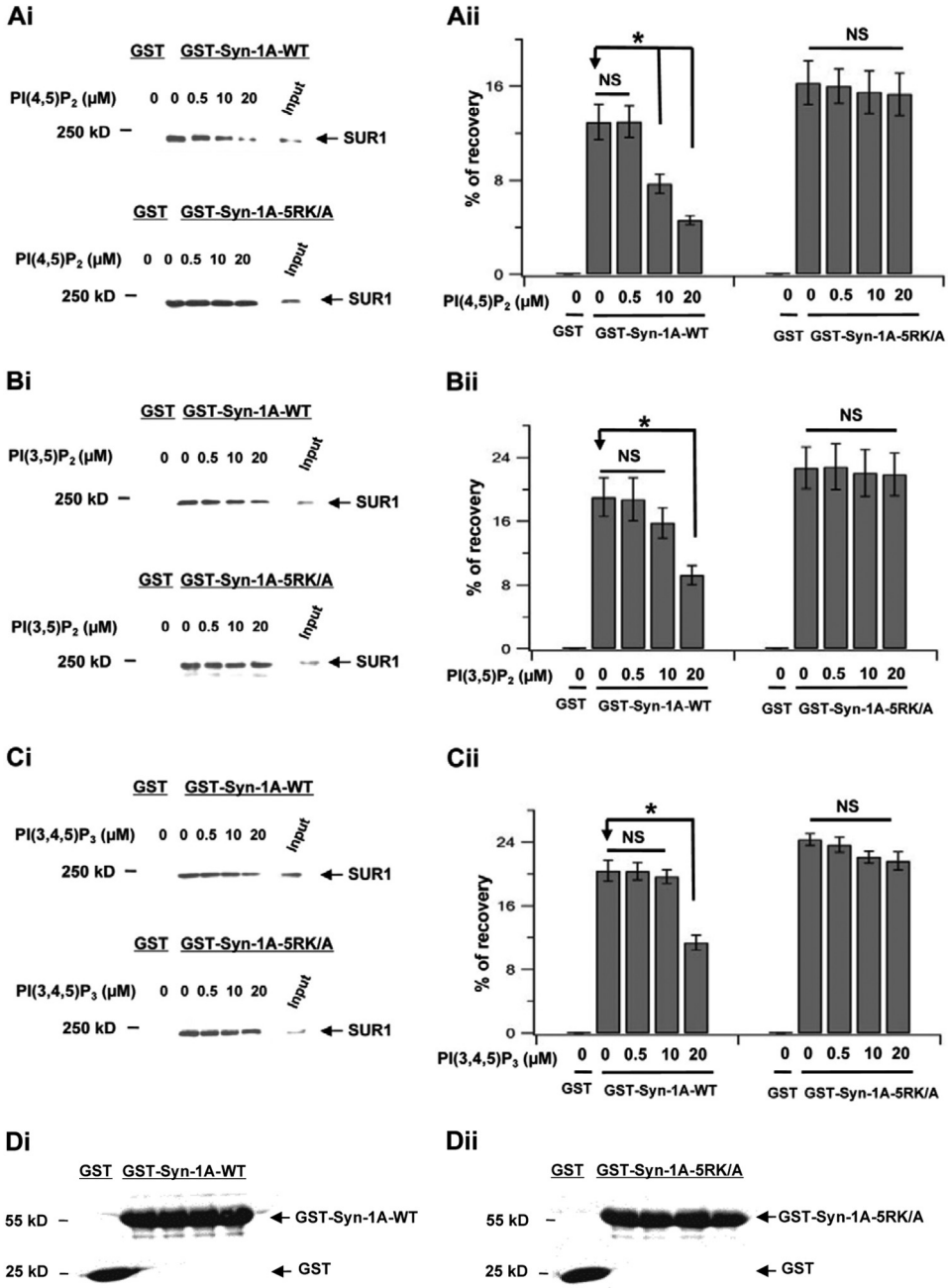

FIGURE 1. **Exogenously added PIP$_2$ disruption of Syn-1A·SUR1 complex formation.** GST-Syn-1A-WT or GST-Syn-1A-5RK/A and GST (as control) were used to pull down SUR1 from HEK293 cells co-transfected with SUR1 and Kir6.2 in presence of indicated concentrations of the following inositol phospholipids: PIP$_2$ (*PI(4,5)P$_2$* in *A*), PI(3,5)P$_2$ (*B*), and PI(3,4,5)P$_3$ (*C*). *i* (in *A–C*), representative blots showing the effects of increasing inositol phospholipids concentrations in disrupting Syn-1A binding to SUR1 (*top*) but not Syn-1A-5RK/A binding to SUR1 (*bottom*). *ii* (in *A–C*), summary of three separate experiments, with each band normalized as a percentage of the input (400-μg protein of HEK cell lysate extract; see "Experimental Procedures"). Data are expressed as mean ± S.E. (*error bars*); *, $p < 0.05$. *NS*, not significant. *D*, 20 μg of protein of GST-Syn-1A or GST-Syn-1A-5RK/A and control GST uniformly used in all of the samples of these experiments was assessed by Ponceau S staining. A representative sample in *D* shows equal amounts used. *i*, GST-Syn-1A WT; *ii*, GST-Syn-1A-5RK/A.

ally recovered the currents to the level observed immediately after patch excision. Consistent with previous reports, prior to PIP_2 applications, both 1 and 3 mM ATP inhibited K_{ATP} channels; however, three subsequent applications of PIP_2 decreased ATP sensitivity and completely abolished the inhibitory effect of 1 mM ATP, as reported previously (14). Of note, Fig. 2*B* shows that concomitant application of GST-Syn-1A and PIP_2 did not completely recover the channels after rundown. In addition, in the presence of GST-Syn-1A, reapplication of ATP after PIP_2 activation did not produce any less current inhibition. In Fig. 2*C*, adding GST-Syn-1A greatly reduced PIP_2-mediated channel activation, causing a rightward shift of the dose response. EC_{50} values for PIP_2 in the absence and presence of GST-Syn-1A are 2.38 ± 0.81 ($n = 5$) and 9.64 ± 0.14 ($n = 3$), respectively. Our results indicate that exogenously added GST-Syn-1A inhibits K_{ATP} channels through direct binding and interaction with SUR1 at its cytoplasmic nucleotide-binding folds (NBF-1 and NBF-2), as we reported previously (34), and that Syn-1A regulates K_{ATP} channels through PIP_2 interactions. For the latter finding, our results suggest that the exoge-

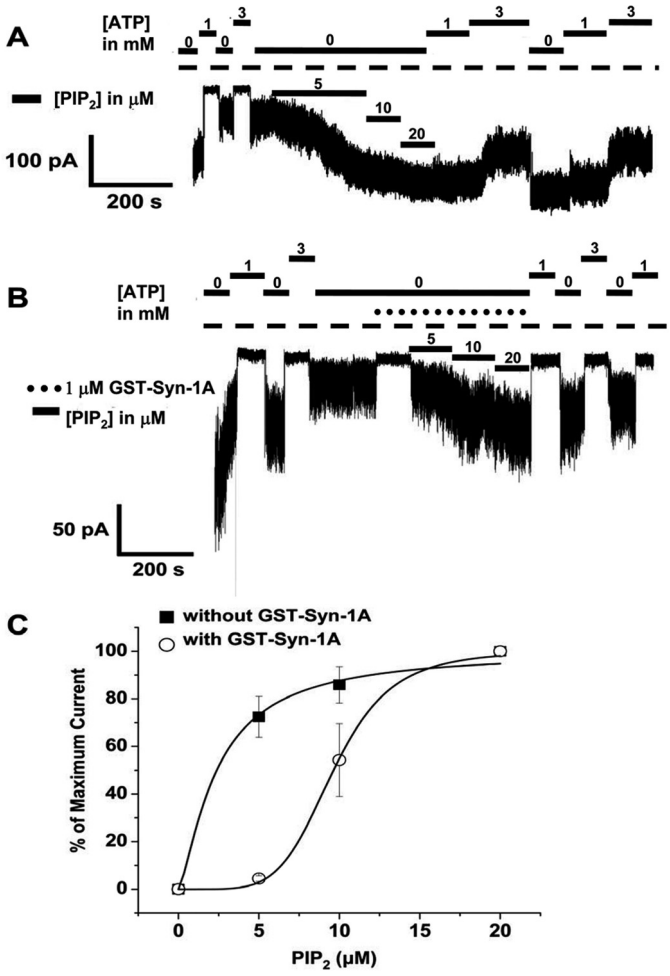

FIGURE 2. **Inside-out patch recording of INS-1 cells showing that PIP$_2$ dose-dependent activation of K$_{ATP}$ channels is reduced by Syn-1A.** Shown are representative traces of the protocol utilized for PIP$_2$ (as shown) in the absence (*A*) or presence (*B*) of 1 μM GST-Syn-1A. Membrane patches were initially exposed to 0, 1, and 3 mM ATP K_{int} solution to characterize K_{ATP} channels and verify the ATP sensitivity of the currents recorded. *C*, PIP$_2$ dose-dependent activation of K_{ATP} current in the absence ($n = 5$) and presence of Syn-1A ($n = 3$). Results are mean ± S.E. (*error bars*).

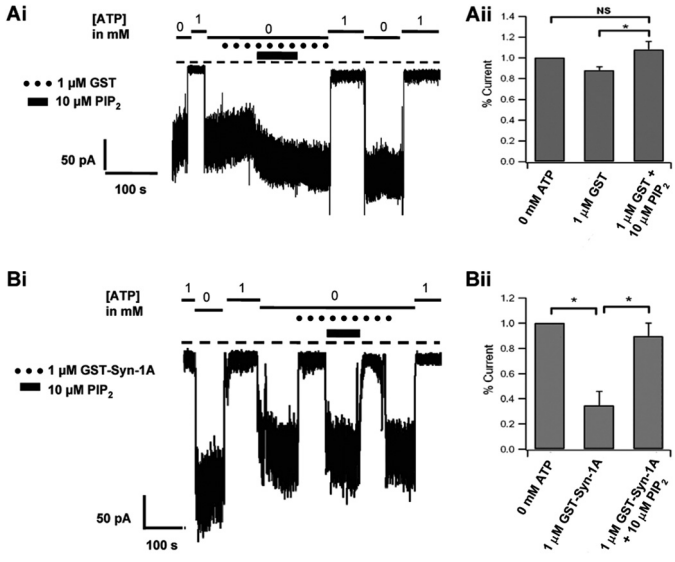

FIGURE 3. **Inside-out patch recording of INS-1 cells showing PIP$_2$ activation K$_{ATP}$ currents exceeds PIP$_2$-mediated recovery of Syn-1A inhibition of K$_{ATP}$ currents.** Representative K_{ATP} current tracings of 1 μM GST with 10 μM PIP$_2$ (*Ai*) and 1 μM GST-Syn-1A with 10 μM PIP$_2$ (*Bi*) and their respective summary data (*Aii* and *Bii*; $n = 5$ cells each) of the maximum current (in 0 mM ATP K_{int} solution). Here, membrane patches were initially exposed to 0 and 1 mM ATP K_{int} solution. Results are mean ± S.E. (*error bars*); *, $p < 0.05$; *NS*, not significant.

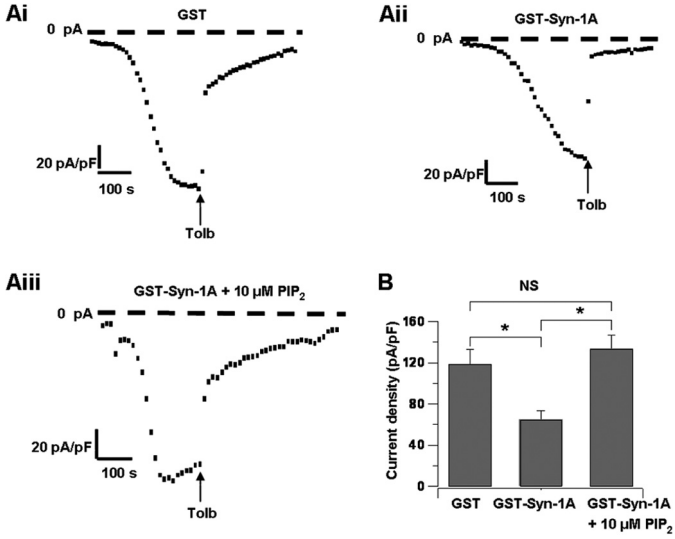

FIGURE 4. **Whole-cell recording of rat islet β-cells showing PIP$_2$ actions on Syn-1A to functionally disrupt Syn-1A·SUR1 interactions.** *A*, representative K_{ATP} currents with 1 μM GST (*i*), 1 μM GST-Syn-1A (*ii*), or 1 μM GST-Syn-1A plus 10 μM PIP$_2$ (*iii*) dialyzed into β-cells. Tolbultamide (Tolb; 0.1 mM) was added to verify the K_{ATP} current. *B*, summary data of *A* showing maximum current density with 1 μM GST ($n = 6$), 1 μM GST-Syn-1A ($n = 8$), or 1 μM GST-Syn-1A plus 10 μM PIP$_2$ ($n = 11$). Results are mean ± S.E. (*error bars*); *, $p < 0.05$.

nous PIP$_2$ bound GST-Syn-1A (as shown in the binding study in Fig. 1*A*) rather than becoming incorporated into the PM to affect endogenous PM-bound Syn-1A. From Fig. 2*C*, we selected 10 μM PIP$_2$ to further study and analyze PIP$_2$-Syn-1A interactions and their effects on K_{ATP} channel activities in the studies in Figs. 3 and 4.

We performed the converse experiment of inside-out recordings of INS-1E cells perfused with GST-Syn-1A (1 μM; indicated by *black circles above* the *current traces*) in the presence or absence of PIP$_2$ (10 μM; indicated by *solid bars*). The summarized results are expressed as percentages of maximum current elicited at 0 mM ATP K_{int} solution determined in each patch. Fig. 3*Ai* shows the representative K_{ATP} current tracing of GST with PIP$_2$, and the corresponding summary data are shown in Fig. 3*Aii* ($n = 5$). Here, K_{ATP} currents underwent spontaneous decay in the absence of ATP; subsequent perfusion of PIP$_2$ in the continuous presence of GST increased channel activities. When comparing K_{ATP} currents between GST alone (87.9 ± 3.62% of control maximal current) and subsequent perfusion of GST and PIP$_2$, PIP$_2$ exposure led to a pronounced increase in K_{ATP} current (108.06 ± 7.77%), which appeared larger but not significantly different from the initial current immediately after patch excision (0 mM ATP K_{int}) (Fig. 2*B*). These results indicate that after patch excision, K_{ATP} channels undergo spontaneous rundown, and subsequent PIP$_2$ exposure led to recovery of channel activity. In Fig. 3, *Bi* and *Bii*), administration of GST-Syn-1A alone reduced maximum control K_{ATP} currents by ~65.4% ($n = 5$). When comparing K_{ATP} currents between GST-Syn-1A alone and subsequent

concomitant perfusion of GST-Syn-1A and PIP_2, PIP_2 recovered Syn-1A-inhibited currents to 89.6 ± 10.52% of maximal currents ($n = 5$), but the currents never reached that seen immediately after patch excision. These results taken together indicate that PIP_2 activation of K_{ATP} currents exceeds PIP_2-mediated recovery of Syn-1A inhibition of K_{ATP} currents. This is probably because of PIP_2 direct actions on the Kir6.2 subunit (12, 13).

PIP_2 Acts on Syn-1A to Functionally Disrupt Syn-1A·SUR1 Interactions in Rat β-Cells—To delineate the physiological relevance of our findings in INS-1E, we employed rat islet β-cells using whole-cell patch clamp recordings. 1 μM GST, 1 μM GST-Syn-1A, or a combination of 1 μM GST-Syn-1A and 10 μM PIP_2 was dialyzed into β-cells via a patch pipette. In the presence of 1 μM GST only (Fig. 4, *Ai* and *B*), K_{ATP} currents gradually developed in β-cells, reaching a maximum current density of 118.97 ± 13.79 pA/pF ($n = 6$). In contrast, dialyzing 1 μM GST-Syn-1A (Fig. 4, *Aii* and *B*) reduced K_{ATP} channel density (65.16 ± 8.62 pA/pF, $n = 8$). In accordance with the aforementioned INS-1E studies, concomitant dialysis of 1 μM GST-Syn-1A and 10 μM PIP_2 (Fig. 4, *Aiii* and *B*) gave a maximum current density of 133.48 ± 13.41 pA/pF ($n = 11$). These results, taken together with the results in Figs. 1–3, suggest that exogenous PIP_2 and GST-Syn-1A seemed to bind and sequester each other from acting on the K_{ATP} channel, with PIP_2 sequestration of GST-Syn-1A disrupting Syn-1A·SUR1 interactions and GST-Syn-1A sequestration of PIP_2 reducing PIP_2 actions on Kir6.2.

PIP_2-insenstive Syn-1A-5RK/A Mutant Reduces PIP_2 Opening of K_{ATP} Channels—Mutations at the Syn-1A juxtamembrane five basic residues (Lys-260, -264, and -265 and Arg-262 and -263), called Syn-1A-5RK/A, rendered Syn-1A PIP_2-insensitive (29). The postulate is that if Syn-1A-5RK/A mutant inhibitory actions on K_{ATP} channels would not be disrupted by PIP_2, then PIP_2 activation of K_{ATP} channels may be reduced. Furthermore, the contribution of Syn-1A inhibitory action on SUR1 may be able to oppose the direct actions of PIP_2 on Kir6.2 in opening the channel.

We first examined the effects of PIP_2 on Syn-1A-5RK/A binding to SUR1 employing two assays, an *in vitro* binding assay (Fig. 1*A*) and *in vivo* FRET assay (Fig. 5). In contrast to PIP_2 dose-dependent disruption of GST-Syn-1A-WT protein binding to SUR1 (in SUR1/Kir6.2-expressing HEK cells), GST-Syn-1A-5RK/A (containing only cytoplasmic domain aa 1–265) binding to SUR1 remained intact (*i.e.* unperturbed by $PI(4,5)P_2$ (Fig. 1*A*), $PI(3,5)P_2$ (Fig. 1*B*), or $PI(3,4,5)P_3$ (Fig. 1*C*)). When the amount of GST-Syn-1A binding to SUR1 was assessed as a percentage of total HEK cell SUR1 input content, it appeared that GST-Syn-1A-5RK/A·SUR1 complexes (16.28 ± 1.86, $n = 3$) were 27% higher than GST-Syn-1A·SUR1 complexes (12.86 ± 1.49; Fig. 1*A*). These results indicate that Syn-1A is able to bind SUR1 tightly *in vitro* in the absence of PIP_2 and that Syn-1A binds SUR1 at other H3 domains (27) outside the PIP_2-binding domain.

The previous studies in Figs. 1–4 examined the effects of exogenously added GST-Syn-1A (containing only the cytoplasmic domain) and PIP_2 on K_{ATP} channels. Live cell FRET imaging analysis enables the examination of full-length Syn-1A-mCherry *versus* full-length Syn-1A-5RK/A-mCherry and SUR1-EGFP expressed in HEK293 cells. Here, we assessed whether PIP_2 can disrupt their *in vivo* (thus physiological) interactions on PM by TIRF imaging (Fig. 5), which optically isolates the PM surface (see "Experimental Procedures"). HEK293 cells were permeabilized with digitonin to permit entry of PIP_2 (10 μM). Of note, the addition of this physiologic PIP_2 concentration seemed to increase the fluorescence intensity of the Syn-1A-mCherry hotspots (indicated by *arrows*), suggesting an increase in Syn-1A-mCherry cluster formation in these PM areas (Fig. 5*A*, *top images*). Remarkably, in the same experiment (Fig. 5*A*, *bottom images*), the 10 μM PIP_2 disrupted Syn-1A·SUR1 complexes (indicated by *arrowheads*), shown as a reduction of FRET efficiency from 30.69 ± 2.2 to 15.381 ± 1.3 (Fig. 5, *A* and *C*). This was a ~50% reduction, which, when taken with the similar disruption of GST-Syn-1A·SUR1 complexes in the protein-binding study (Fig. 1*A*), suggests that PIP_2 disruption of Syn-1A·SUR1 complexes seems to "free" more Syn-1A molecules to participate in the formation of Syn-1A clusters, the latter also promoted by PIP_2. Remarkably, PIP_2 did not disrupt Syn-1A-5RK/A·SUR1 complexes (indicated by *arrowheads* in Fig. 5*B*; no PIP_2, 37.14 ± 3.1; with PIP_2, 35.42 ± 1.7 (Fig. 5*C*)). We noted larger areas of Syn-1A-5RK/A·SUR1 FRET fluorescence (Fig. 5*B*) than Syn-1A·SUR1 fluorescence (Fig. 5*A*, *bottom*). Thus, we calculated the fluorescent area against total PM area (Fig. 5*D*) and found that the Syn-1A-RK/A·SUR1 FRET area occupied 31.9 ± 4.9%, which is 198% of the Syn-1A·SUR1 FRET area of 16.1 ± 3.7%. Along with the binding studies in Fig. 1*A*, it seems that the Syn-1A-5KR/A mutation increased its abundance on the PM from increased formation of Syn-1A-5RK/A·SUR1 complexes. Last, we noticed that the locations of Syn-1A·SUR1 FRET signals (Fig. 5*A*, *bottom*; indicated by *arrowheads*) were mostly not colocalized with the areas with abundant Syn-1A-mCherry (Fig. 5*A*, *top* and *bottom*; indicated by *arrows*), an important point that we discuss further below along with the results in Fig. 9. In these studies, we were a little surprised by these strongly positive results because we had initially expected that exogenously added PIP_2 would not incorporate substantially into the PM (30), thus exhibiting lesser effects on the Syn-1A·SUR1 interactions in the PM. The most likely explanation is that PIP_2 incorporates into PM through lipid tails over time, which would occur with greater frequency the longer duration PIP_2 in solubilized solution is exposed to the interior surface of the cell. Another explanation is that digitonin (used for permeabilization) affects PM cholesterol in a manner that could influence PIP_2 incorporation into PM or increase the sensitivity to PIP_2 promotion of Syn-1A cluster formation in the PM (21, 22). Digitonin permeabilization (prior to the addition of PIP_2), however, did not independently affect Syn-1A cluster formation or Syn-1A·SUR1 FRET interactions (Fig. 5*A*). Alternatively, PM permeabilization might have led to inadvertent depletion of some cytosolic factors that can influence the state of Syn-1A (free *versus* complexed) or the sensitivity of Syn-1A·SUR1 complex disruption by PIP_2.

We then determined the functional implications of these binding studies by examining whether PIP_2 activation of K_{ATP} channels in INS-1 cells would be perturbed by the PIP_2-insenstive mutation of Syn-1A. As shown in Fig. 6*A* (analysis in Fig.

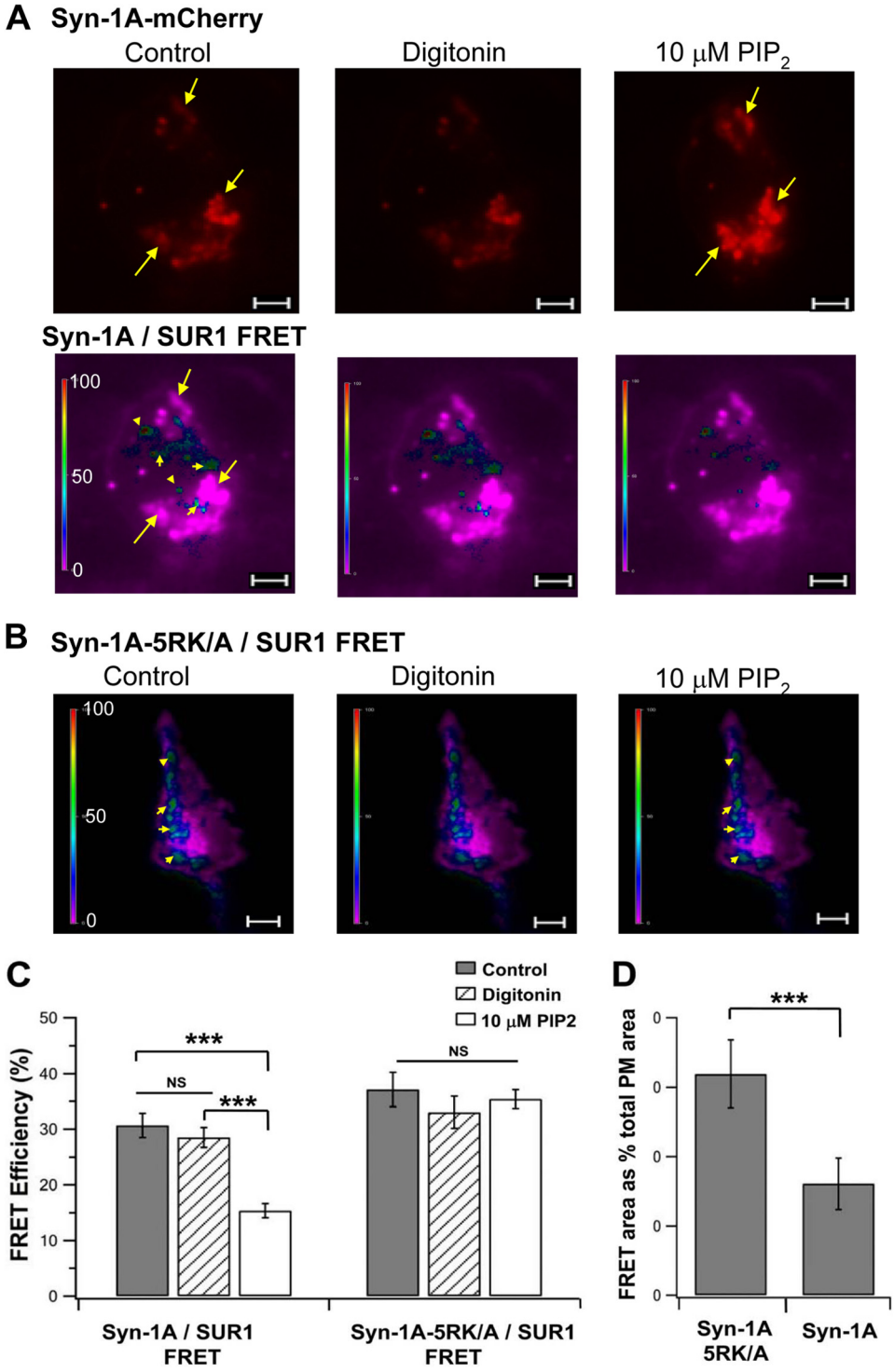

FIGURE 5. ***In vivo* TIRFM FRET imaging showing that PIP$_2$ disrupts Syn-1A WT but not PIP$_2$-insensitive Syn-1A-5RK/A binding to SUR1.** Shown in *A* and *B* are representative recordings of FRET signals on the PM (indicated by different *pseudocolors*) of HEK cell expressing WT-Syn-1A-mCherry (*A*) or Syn-1A-5RK/A-mCherry (*B*), SUR1-EGFP, and Kir6.2 prior to (control) and after the addition of 10 μM PIP$_2$ to the permeabilized cells. In *A*, the Syn-1A-mCherry fluorescent images are also shown (*top images*). *Arrows* in *A*, Syn-1A-mCherry hotspots; *arrowheads* in *A* and *B*, FRET hotspots. *Scale bar*, 5 μm. A *vertical scale bar* indicates FRET efficiency in *pseudocolor*. *C*, summary of FRET efficiency represented by images in *A* ($n = 17$) and *B* ($n = 13$). *D*, percentage of FRET fluorescent area on PM as a percentage of total PM area under control conditions ($n = 13$). Results are mean ± S.E. (*error bars*); ***, $p < 0.001$; *NS*, not significant.

6*C*), dialyzing INS-1 cells with standard pipette solution displayed a K_{ATP} channel current density of 100.3 ± 18.7 pA/pF (−140 mV stimulation, used as control in Fig. 6*C*). Under identical conditions, overexpression of full-length Syn-1A-WT plasmid in INS-1 cells (Fig. 6*A*, *left traces*) reduced K_{ATP} channel current density to 29% (29.1 ± 4.2 pA/pF; Fig. 6*C*) of control. Application of 1 μM PIP$_2$ (a physiologically lower concentration than 10 μM PIP$_2$ used in previous binding and functional studies) blunted the overexpressed Syn-1A inhibition to 60% of control (60.2 ± 5.4 pA/pF). In contrast, overexpression of Syn-

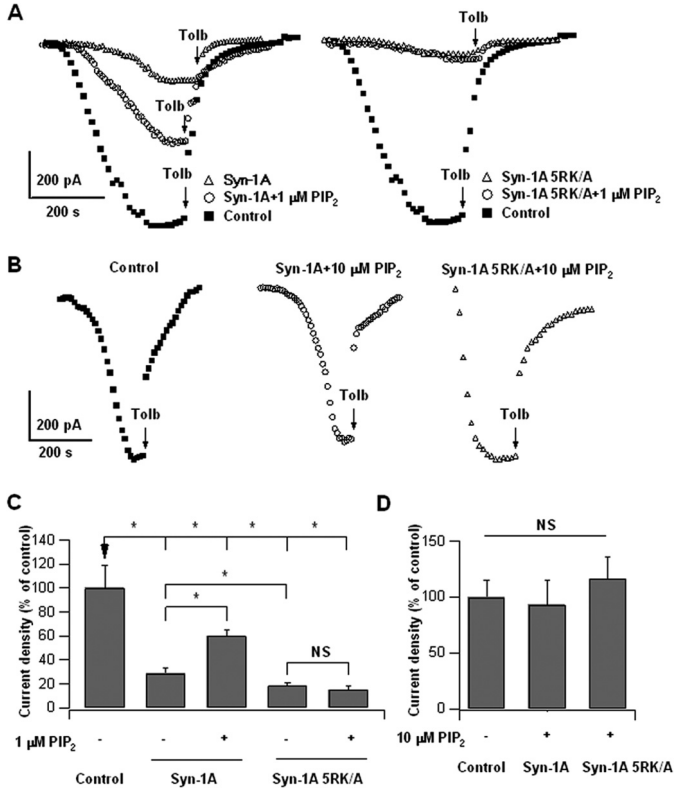

FIGURE 6. **Syn-1A-5RK/A inhibition of K$_{ATP}$ channels is resistant to physiologic low PIP$_2$ (1 μM) but not high PIP$_2$ (10 μM) opening of K$_{ATP}$ channels.** *A*, representative K$_{ATP}$ channel current tracings of Syn-1A-WT- (*left traces*) and PIP$_2$-insensitive Syn-1A-5RK/A-expressing INS-1 cells (*right traces*), treated with or without 1 μM PIP$_2$ (in pipette solution). Note PIP$_2$ partial reversal of Syn-1A inhibition (*left traces*) but not of Syn-1A-RK/A inhibition (*right traces*). *B*, representative K$_{ATP}$ channel current traces from control (*left*), Syn-1A WT (*middle*), and Syn-1A-5RK/A (*right*)-overexpressing INS-1 cells treated without or with 10 μM PIP$_2$ (in pipette solution). *C*, summary of *A*, $n = 6$–12 cells. *D*, summary of *B* showing no difference in current densities between control ($n = 8$), Syn-1A WT-expressing ($n = 9$), and Syn-1A-5RK/A-expressing ($n = 11$) cells. Results are mean ± S.E. (*error bars*); *, $p < 0.05$; *NS*, not significant.

1A-5RK/A (Fig. 6*A*, *right traces*; analysis in Fig. 6*C*) into INS-1 cells reduced K$_{ATP}$ channel current to 18.6% of control (18.6 ± 2.1 pA/pF), which was a further 36% reduction from that caused by overexpressed Syn-1A ($p < 0.05$). This more potent inhibition of K$_{ATP}$ channel activity by Syn-1A-5RK/A is consistent with increased Syn-1A-5RK/A·SUR1 complex formation in PM (Figs. 1 and 5*D*). Remarkably, the addition of 1 μM PIP$_2$ could not increase K$_{ATP}$ current inhibited by overexpressed Syn-1A-5RK/A (14.9 ± 3.1 pA/pF; Fig. 6*A*, *right traces*; analysis in Fig. 6*C*).

The above results suggest that under physiologically low PIP$_2$ concentration (~1 μM), PIP$_2$ modulation of Syn-1A·SUR1 complex was sufficient to modulate K$_{ATP}$ activity, which seemed more dominant over the direct actions of PIP$_2$ on Kir6.2 to open channels. In this experiment, the exogenous PIP$_2$ was acting directly on the cytoplasmic PIP$_2$-binding domain of Syn-1A and not likely to have significantly affected Syn-1A cluster formation in PM. Importantly, a 1 μM PIP$_2$ concentration had no detectable effect on Syn-1A·SUR1 complex assembly, at least *in vitro*, which may in part be due to differences in the sensitivity of the assay (Fig. 1*A*). When we raised PIP$_2$ concentration to 10 μM (which disrupted *in vitro* Syn-1A·SUR1 assembly in Fig. 1*A*), we found no differences in K$_{ATP}$ channel activities between control, Syn-1A-WT, and Syn-1A-5RK/A (Fig. 6*B*; analysis in Fig. 6*D*). These results indicate that at higher PIP$_2$ concentration, direct effects of PIP$_2$ on the Kir6.2 subunit predominate over the effects of PIP$_2$ on Syn-1A-5RK/A(and Syn-1A-WT) and SUR1 interaction to open K$_{ATP}$ channels, although this higher PIP$_2$ dosage remained unable to disrupt the abundant Syn-1A-5RK/A·SUR1 complexes (Figs. 1*A* and 5, *C*–*E*). These results modified our original thinking to suggest several modes by which PIP$_2$ activates K$_{ATP}$ channels in insulin-secreting β-cells: one at physiologic low PIP$_2$ concentration acting on Syn-1A at its PIP$_2$-binding site that finely modulates Syn-1A·SUR1 interactions and one at higher PIP$_2$ concentrations, which act on K$_{ATP}$ channels by two mechanisms, first by directly binding Kir6.2 and second by sequestering Syn-1A molecules into Syn-1A clusters, which reduces the availability of free Syn-1A molecules to bind SUR1 and could disrupt Syn-1A·SUR1 complexes.

Specificity of Cellular Inositol Phospholipids in Modulating Syn-1A·SUR1 Complex Disassembly and K$_{ATP}$ Channel Activity—We next assessed whether other abundant cellular phospholipids might similarly affect Syn-1A·SUR1 complexes (Fig. 7) to modify K$_{ATP}$ channel activity (Fig. 8) and whether this is mainly attributable to the negative charge of phospholipids purported to bind positively charged juxtamembrane polybasic residues of Syn-1A (14, 35, 36). FRET imaging assessment showed that 10 μM phosphatidylcholine (0 net charge) and phosphatidyl-L-serine (less negative charge than PIP$_2$) did not affect Syn-1A·SUR1 complex formation (Fig. 7, *A*, *B*, and *D*) or HEK293 K$_{ATP}$ channel activities (Fig. 8, *A*, *B*, *C*, and *E*). Inositol trisphosphate (IP$_3$), which has a larger negative charge compared with PIP$_2$ (38), caused only a minor disruption (24%) in Syn-1A·SUR1 complexes (Fig. 7, *C* and D; without IP$_3$, 33.05 ± 2.9; with IP$_3$, 24.91 ± 3.9) but did not significantly affect K$_{ATP}$ channel activity (Fig. 8, *D* and *E*). These results indicate that the PIP$_2$ effects on Syn-1A·SUR1 interactions that modulate K$_{ATP}$ channel activity are specific.

Effects of PIP$_2$ Depletion from PM on Syn-1A·SUR1 Complex Formation and K$_{ATP}$ Channels—Our experiments above so far have used exogenous PIP$_2$ to alter Syn-1A·SUR1 interactions. Synaptojanin-1 is a polyphosphoinositide 5-phosphatase, which, when overexpressed using the construct HA-IPP1-CAAX, was reported to deplete endogenous PIP$_2$ from the PM, causing disruption of the Syn-1A clusters on the PM (30, 31). Consistently, expressing this synaptojanin-1 construct to deplete endogenous PIP$_2$ (in Fig. 9*A*), we saw a reduction of the larger hotspots (suggesting clusters, indicated by *arrowheads* in the *top images*) of Syn-1A-mCherry fluorescence (Syn-1A-mCherry expressed in HEK cells) to small fluorescence spots (indicated by *arrowheads* in the *bottom images*), indicating a dispersion of Syn-1A molecules from Syn-1A clusters; this is similar to the previous report using this construct (31). Further intensity profile analysis of cross-sections of the indicated regions of these images shows that in the absence of synatojanin-1 (Fig. 9*B*, *pink line*), there was sustained high intensity Syn-1A-mCherry fluorescence suggesting Syn-1A clusters, whereas in the cell treated with synaptojanin-1, Syn-1A-mCherry fluorescence appeared as *narrow spikes*, indicating either dispersed Syn-1A molecules

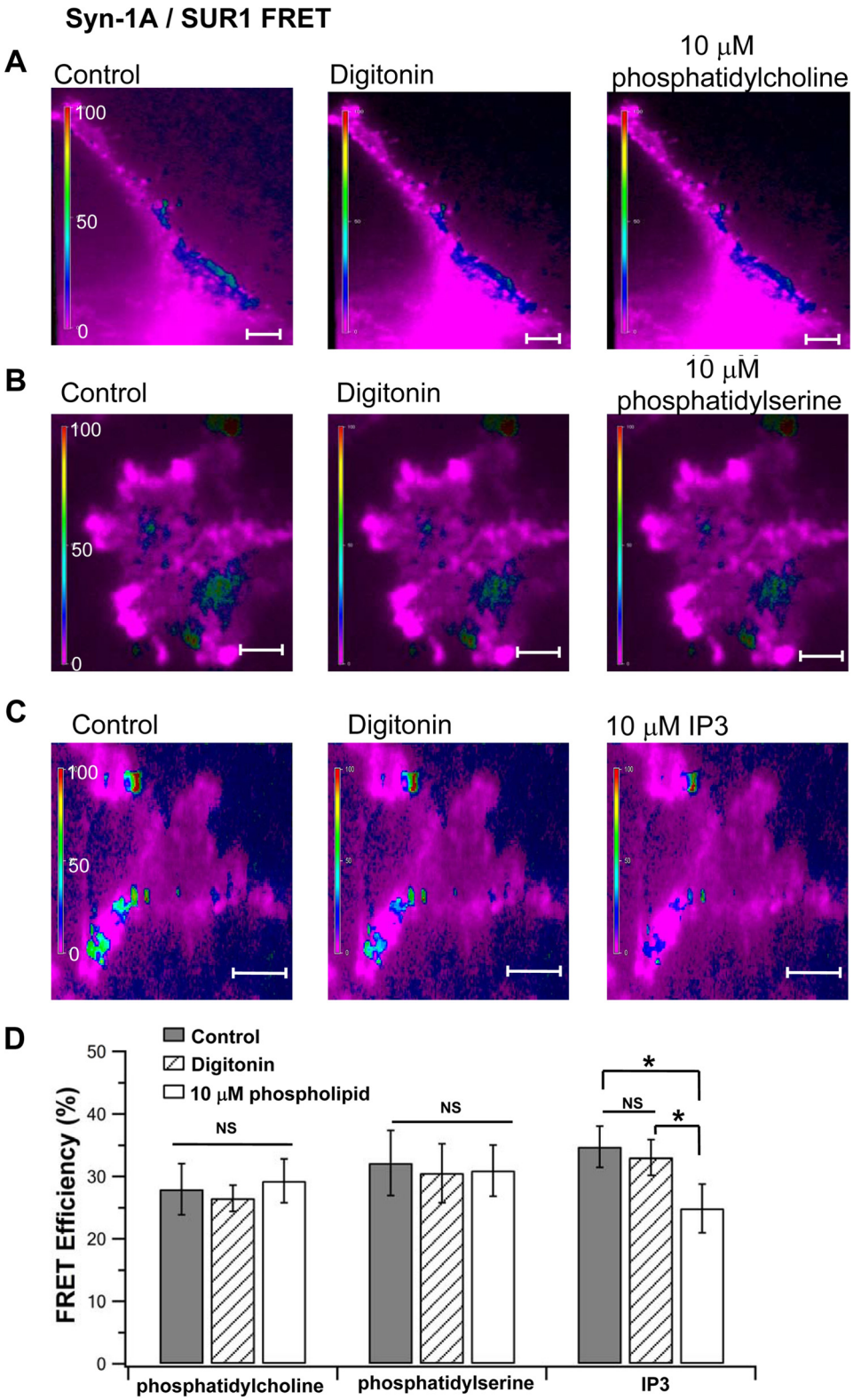

FIGURE 7. ***In vivo* FRET TIRFM imaging showing other phospholipids had little or no effect on Syn-1A·SUR1 complexes.** 10 μM phosphatidylcholine (*A*), phosphatidyl-L-serine (*B*), and IP$_3$ (*C*) were added to digitonin-permeabilized HEK cells expressing WT-Syn-1A-mCherry and SUR1-EGFP (as in Fig. 5). Shown are representative cells for each condition. *D*, summary of FRET efficiency (mean ± S.E. (*error bars*)) of *A* ($n = 14$), *B* ($n = 13$), and *C* ($n = 15$). *, $p < 0.01$; *NS*, not significant.

or much smaller clusters of Syn-1A molecules (Fig. 9*C*, *blue line*). These results are consistent with Fig. 5*A* (*top images*), where the addition of exogenous PIP$_2$ appeared to increase Syn-1A-mCherry clustering on PM. Synaptojanin-1-induced depletion of endogenous PIP$_2$ resulted in increased FRET signals (59.3 ± 6.2%; Fig. 9*D*) compared with the absence of synaptojanin-1 (35.6 ± 7.1%; note more *green* to *red* in +synpatojanin-1 *versus blue* to *green* in −synaptojanin-1 in Fig. 9*A*), indi-

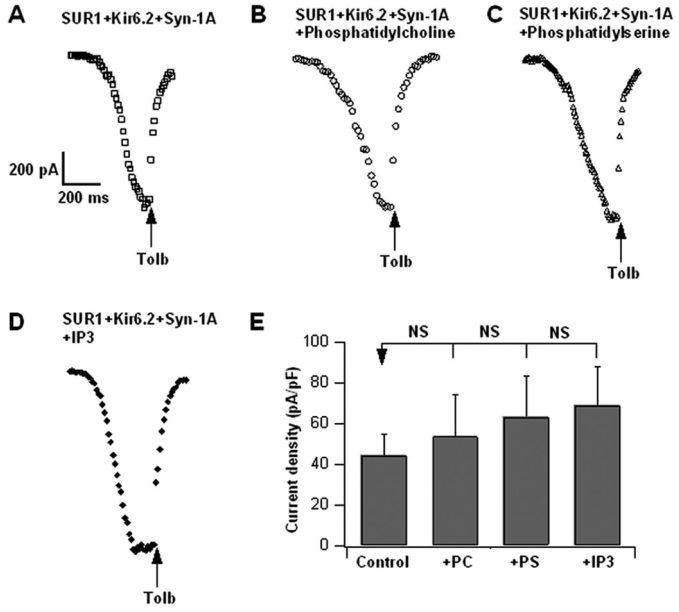

FIGURE 8. **WT Syn-1A inhibition of K_{ATP} channels is resistant to other phospholipids.** Representative K_{ATP} channel current tracings of SUR1 + Kir6.2 + Syn-1A-WT-expressing HEK293 cells, control (*A*) or treated with 10 μM phosphatidylcholine (*B*), phosphatidyl-L-serine (*C*), or inositol 1,4,5-trisphosphate (IP_3) (*D*) in the pipette solution. *E*, summary showing no difference in current densities between control cells ($n = 7$) and each of the phospholipid-treated cells (phosphatidylcholine, $n = 6$; phosphatidyl-L-serine, $n = 6$; IP_3, $n = 6$). Results are means ± S.E. (*error bars*); *NS*, not significant.

cating increased Syn-1A·SUR1 complex formation in the PM. Of note, in −synaptojanin-1 cells, the FRET signals (indicated by *arrows*) were mostly located away from the Syn-1A-mCherry clusters (indicated by *arrowheads*; Fig. 9*A*), as was similarly observed in Fig. 5*A*. In contrast, in +synaptojanin-1 cells, the FRET signals were mostly in small Syn-1A-mCherry hotspots (*arrows* and *arrowheads* point to the same hotspots). These results led us to further strengthen our thinking that PIP_2 depletion releases Syn-1A molecules from the large Syn-1A clusters to migrate away from the cluster to other PM sites where SUR1 molecules are located to then form Syn-1A·SUR1 complexes.

We then examined the functional implications of the endogenous PIP_2 depletion that we showed to increase Syn-1A·SUR1 complex formation. In Fig. 10, *A* and *B*, INS-1 cells transfected with synaptojanin-1 caused a 63% reduction of K_{ATP} current, from 148.35 ± 23.2 pA/pF (control, $n = 7$) to 55.38 ± 11.2 pA/pF (synaptojanin-1, $n = 9$; $p < 0.01$). The application of exogenous GST-Syn-1A (1 μM) to the synaptojanin-1-transfected cells showed a K_{ATP} current of 51.54 ± 9.3 pA/pF ($n = 7$; $p < 0.05$), which is a 65% reduction compared with control. This is very similar to the effects of synaptojanin-1 treatment alone, indicating that exogenously added GST-Syn-1A could not further reduce the K_{ATP} current that was already inhibited by the PIP_2 depletion caused by synaptojanin-1 treatment. Taken together, these results suggest that the enhanced "endogenous" Syn-1A·SUR1 complex formation caused by PIP_2

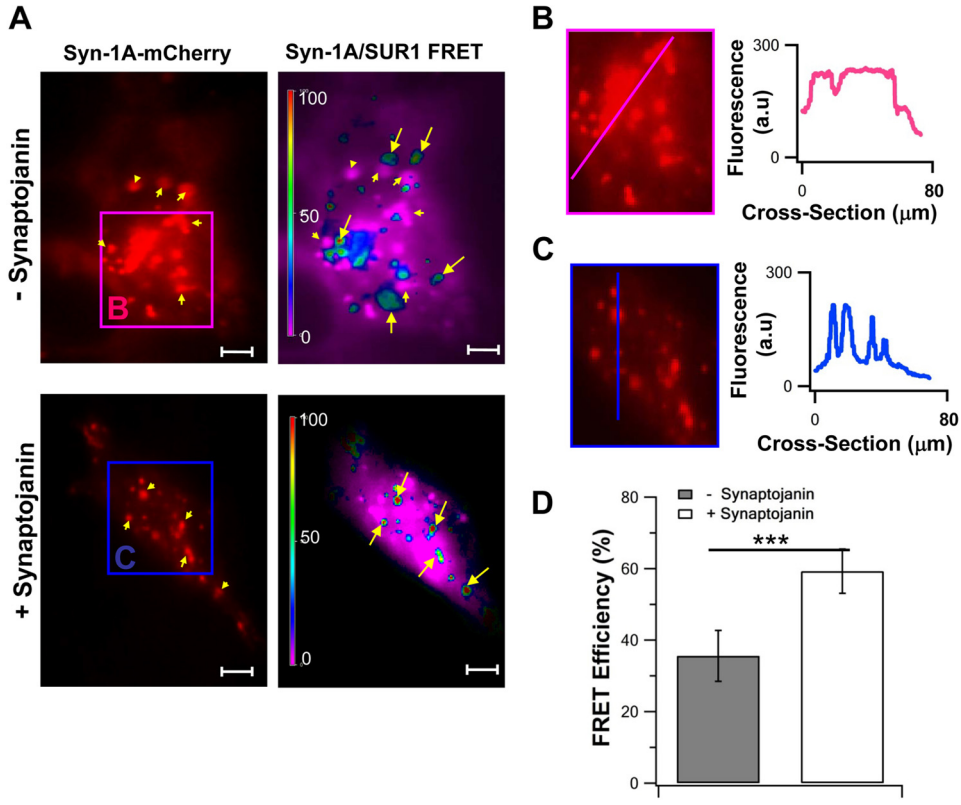

FIGURE 9. **TIRFM FRET imaging showing that PIP_2 depletion from PM disperses Syn-1A clusters, releasing Syn-1A to form complexes with SUR1.** *A*, representative image recordings of Syn-1A-mCherry and corresponding FRET signals on the PM (indicated by different *pseudocolors*) of HEK293 cells expressing Syn-1A-mCherry, SUR1-EGFP, and Kir6.2. The *top images* show that Syn-1A-mCherry (indicated by *arrowheads*) clustered in microdomains (*region B*; *pink box*). Synaptojanin-1 expression to reduce endogenous PIP_2 levels (*bottom images* in *A*) dispersed Syn-1A clusters into smaller Syn-1A-mCherry hotspots (*region C*; *blue box*). *B* and *C*, magnifications of the indicated regions in (*A*), wherein we analyzed the intensity profile of the cross-sections along the *pink* and *blue lines*, shown in the *graphs* on the *right*. *D*, summary of FRET efficiency represented by images in *A* (mean ± S.E. (*error bars*), $n = 14$ cells for each group; ***, $p < 0.001$).

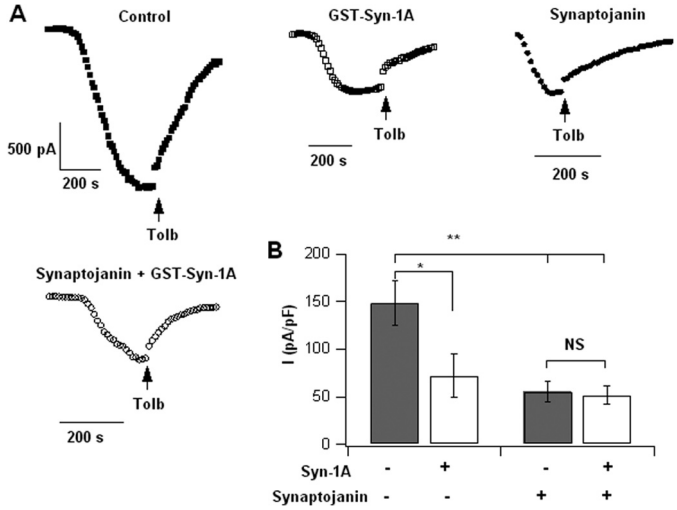

FIGURE 10. **PIP$_2$ depletion from PM disables exogenous Syn-1A from further inhibiting K$_{ATP}$ channels.** *A*, representative K$_{ATP}$ channel current tracings of control, GST-Syn-1A (1 μM infused into cells via patch pipette), synaptojanin-1, and synaptojanin + GST-Syn-1A in INS-1 cells. *B*, summary results showing that exogenous GST-Syn-1A could not cause further inhibition of K$_{ATP}$ channels when endogenous PIP$_2$ levels were depleted by synaptojain-1. Results are mean ± S.E.; *, $p < 0.05$; **, $p < 0.01$. *NS*, not significant.

depletion must have had all of the SUR1 sites occupied by endogenous Syn-1A to have resulted in optimal inhibition of K$_{ATP}$ channels, leaving no available SUR1 sites for the exogenous GST-Syn-1A to bind and further inhibit K$_{ATP}$ channels.

DISCUSSION

In this work, we showed that the actions of PIP$_2$ on activating pancreatic islet β-cell K$_{ATP}$ channel are contributed by alteration of Syn-1A interactions with SUR1, in addition to the known actions of PIP$_2$ on Kir6.2 (14–18, 35, 36). Specifically, we showed that *in vitro* binding of recombinant GST-Syn-1A (containing only the cytoplasmic domain) and SUR1 was dose-dependently disrupted by increasing PIP$_2$ concentrations (Fig. 1*A*). Although these results suggest that exogenous GST-Syn-1A and PIP$_2$ could sequester each other from acting on K$_{ATP}$ channels, our FRET study showed that PIP$_2$ could also disrupt *in vivo* FRET interactions of SUR1 (-EGFP) and full-length Syn-1A (-mCherry) (Fig. 5). PIP$_2$ effects on Syn-1A·SUR1 interactions were relatively specific at physiologic concentrations, with similar charged PI(3,5)P$_2$ having reduced effects and more (PIP$_3$) or less negatively charged phospholipids having little to no effect on Syn-1A·SUR1 complex assembly or K$_{ATP}$ channel activity (Figs. 1 (*B* and *C*), 7, and 8). The functional implication of GST-Syn-1A·SUR1 sequestration was demonstrated by electrophysiological studies on rat islet β-cells, INS-1E cells, and SUR1/Kir6.2-expressing HEK293 cells, which uniformly showed that efficacy of PIP$_2$ activation of K$_{ATP}$ channels could be reduced by the addition of GST-Syn-1A (Figs. 2–4). All of these effects of PIP$_2$ on Syn-1A·SUR1 complex formation and consequent K$_{ATP}$ channel activity could be abrogated by the PIP$_2$-insensitive Syn-1A mutant, Syn-1A-5RK/A. Importantly, we demonstrated multiple modes by which PIP$_2$ activates β-cell K$_{ATP}$ channel, whereby modulation of Syn-1A·SUR1 complex formation by physiologic low PIP$_2$ concentration sufficient to alter K$_{ATP}$ channel activity seemed to be more sensitive than the direct actions of PIP$_2$ (at higher concentration) on Kir6.2 (Fig. 6). These results suggest three mechanisms for the actions of the exogenous PIP$_2$ in opening K$_{ATP}$ channels. First, PIP$_2$ binds and sequesters exogenous GST-Syn-1A from binding SUR1. Second, some PIP$_2$ is incorporated into the PM to disrupt Syn-1A·SUR1 complexes in the PM. Third, PIP$_2$ acts on Kir6.2. The release of PM-bound Syn-1A molecules from PIP$_2$-induced disruption of Syn-1A·SUR1 complexes seemed to contribute to the availability of Syn-1A to participate in the increase in Syn-1A clustering on the PM (Fig. 5*A*). This was assessed more critically with experiments whereby we depleted endogenous PIP$_2$ from the PM with synaptojanin-1, reported to reduce Syn-1A clustering on PM (31). Here, endogenous PIP$_2$ depletion appeared to release Syn-1A molecules from the PM clusters (Fig. 9). The "freed" Syn-1A molecules could then migrate to, find, and bind SUR1 molecules to form tight Syn-1A·SUR1 complexes (Fig. 9), which effected optimal inhibition of K$_{ATP}$ channels, leaving no available SUR1 molecules for additional exogenous GST-Syn-1A to bind and further inhibit K$_{ATP}$ channels (Fig. 10).

In our *in vitro* binding studies employing GST-Syn-1A binding to expressed SUR1, the GST-Syn-1A (without the transmembrane domain) would not be expected to form physiologic Syn-1A clusters, but nonetheless the PIP$_2$-binding site at the cytoplasmic aa 260–265 domain directly binds SUR1, and the resulting GST-Syn-1A·SUR1 complex could be disrupted by exogenously added physiologic PIP$_2$ concentrations. These results raise the question of how PIP$_2$ modulation of Syn-1A interactions with SUR1 could influence K$_{ATP}$ channel opening kinetics. We recently reported that Syn-1A binds SUR1 domains at the W$_B$ motif of NBF-1 and W$_A$ and W$_B$ motifs of NBF-2 (33). This suggests that Syn-1A might be binding the NBF-1/-2 dimer rather intimately, perhaps as a scaffolding protein, and this configuration and as yet undefined sites within these binding interfaces of SUR1 with Syn-1A might be putative sites for PIP$_2$ disruption. Although we do not know what the PIP$_2$-sensitive sites are in SUR1, the PIP$_2$-sensitive site in Syn-1A is known (29). We directly tested the latter by employing PIP$_2$-insensitive mutations of the juxtamembrane basic residues in Syn-1A (Syn-1A-5RK/A) (29), and indeed, PIP$_2$ could not disrupt Syn-1A-5RK/A·SUR1 complexes. This was demonstrated by *in vitro* and *in vivo* (FRET) binding studies. The fact that abrogating mutations of the PIP$_2$-binding sites actually increased Syn-1A·SUR1 binding indicates that the Syn-1A can bind SUR1 in a PIP$_2$-independent manner via other H3 domains (27). Consistently, Syn-1A-5RK/A inhibition of SUR1/Kir6.2 K$_{ATP}$ channels was rendered more resistant to PIP$_2$ activation, indicating that the actions of PIP$_2$ on SUR1 via Syn-1A binding have an important contribution to channel opening kinetics. Moreover, we found that PIP$_2$ at 1 μM, which did not disrupt Syn-1A·SNARE complexes could already modulate Syn-1A·SUR1 complex actions on β-cell K$_{ATP}$ channel activity. This was lower than the PIP$_2$ concentrations required to disrupt Syn-1A·SUR1 complexes, and PIP$_2$ with this lower concentration could also directly act on Kir6.2 to induce channel activation. Interestingly, a recent study showed that the N-terminal TMD0 domain of SUR1 profoundly influenced Kir6.2 channel sensitivity to PIP$_2$ (16), which, however, is a domain

that does not bind Syn-1A[5] but which nonetheless could still affect the more distant NBF domains' interactions with Syn-1A.

Hence, we conclude that the PIP_2 effects on SUR1 proteins that influence K_{ATP} channel gating are both direct and indirect. The direct effects we showed in this work are PIP_2 actions on Syn-1A binding to SUR1, probably at the NBF domains (26, 28). The indirect effects would be PIP_2 actions on Syn-1A clusters on the PM, whereby a physiologic increase or reduction of PM PIP_2 levels will determine how many Syn-1A molecules will be released from the Syn-1A clusters to bind adjacent SUR1 molecules on the PM.

K_{ATP} channels play a most important role in regulating insulin secretion from islet β-cells (4, 5). Thus, any factor that acts directly or indirectly on β-cell K_{ATP} channels could have consequential effects on insulin secretion, which we now show to include PIP_2 actions on Syn-1A binding to SUR1. PM and cytosolic PIP_2 levels are likely to be perturbed in diabetes, metabolic syndrome, and lipid disorders. Syn-1A levels are severely reduced in islets of type-2 diabetic patients (39). Because the electrostatic binding between PIP_2 and Syn-1A might enable each to sequester the other (21, 22), the excess or deficiency of either one in these pathologic conditions could profoundly influence the availability of Syn-1A to bind SUR1 or the availability of PIP_2 to bind Kir6.2. Thus, this combined perturbation of β-cellular lipids and Syn-1A levels would probably contribute to perturbation of K_{ATP} channels that in turn could partly account for the deficient biphasic insulin secretion in diabetes.

REFERENCES

1. Aittoniemi, J., Fotinou, C., Craig, T. J., de Wet H., Proks, P., and Ashcroft, F. M. (2009) Review. SUR1. A unique ATP-binding cassette protein that functions as an ion channel regulator. *Philos. Trans. R. Soc. Lond. B Biol. Sci.* **364,** 257–267
2. Aguilar-Bryan, L., and Bryan, J. (1999) Molecular biology of adenosine triphosphate-sensitive potassium channels. *Endocr. Rev.* **20,** 101–135
3. Nichols, C. G., Shyng, S. L., Nestorowicz, A., Glaser, B., Clement, J. P., 4th, Gonzalez, G., Aguilar-Bryan, L., Permutt, M. A., and Bryan, J. (1996) Adenosine diphosphate as an intracellular regulator of insulin secretion. *Science* **272,** 1785–1787
4. Hou, J. C., Min, L., and Pessin, J. E. (2009) Insulin granule biogenesis, trafficking and exocytosis. Vitamins and hormones. *Vitam. Horm.* **80,** 473–506
5. Ashcroft, F. M., and Gribble, F. M. (1999) Differential sensitivity of beta-cell and extrapancreatic K(ATP) channels to gliclazide. *Diabetologia* **42,** 903–919
6. Rohács, T., Lopes, C. M., Jin, T., Ramdya, P. P., Molnár, Z., and Logothetis, D. E. (2003) Specificity of activation by phosphoinositides determines lipid regulation of Kir channels. *Proc. Natl. Acad. Sci. U.S.A.* **100,** 745–750
7. Kwiatkowska, K. (2010) One lipid, multiple functions. How various pools of PI(4,5)P(2) are created in the plasma membrane. *Cell Mol. Life Sci.* **67,** 3927–3946
8. Cremona, O., and De Camilli, P. (2001) Phosphoinositides in membrane traffic at the synapse. *J. Cell Sci.* **114,** 1041–1052
9. Hilgemann, D. W., Feng, S., and Nasuhoglu, C. (2001) The complex and intriguing lives of PIP2 with ion channels and transporters. *Sci. STKE* **2001,** re19
10. Czech, M. P. (2000) PIP_2 and PIP_3. Complex roles at the cell surface. *Cell* **100,** 603–606
11. Martin, T. F. (2001) PI(4,5)P(2) regulation of surface membrane traffic. *Curr. Opin. Cell Biol.* **13,** 493–499
12. Haider, S., Tarasov, A. I., Craig, T. J., Sansom, M. S., and Ashcroft, F. M. (2007) Identification of the PIP2-binding site on Kir6.2 by molecular modelling and functional analysis. *EMBO J.* **26,** 3749–3759
13. Fan, Z., and Makielski, J. C. (1997) Anionic phospholipids activate ATP-sensitive potassium channels. *J. Biol. Chem.* **272,** 5388–5395
14. Baukrowitz, T., Schulte, U., Oliver, D., Herlitze, S., Krauter, T., Tucker, S. J., Ruppersberg, J. P., and Fakler, B. (1998) PIP2 and PIP as determinants for ATP inhibition of KATP channels. *Science* **282,** 1141–1144
15. Enkvetchakul, D., Loussouarn, G., Makhina, E., Shyng, S. L., and Nichols, C. G. (2000) The kinetic and physical basis of K(ATP) channel gating. Toward a unified molecular understanding. *Biophys. J.* **78,** 2334–2348
16. Pratt, E. B., Tewson, P., Bruederle, C. E., Skach, W. R., Shyng, S. L. (2011) N-terminal transmembrane domain of SUR1 controls gating of Kir6.2 by modulating channel sensitivity to PIP2. *J. Gen. Physiol.* **137,** 299–314
17. Stansfeld, P. J., Hopkinson, R., Ashcroft, F. M., and Sansom, M. S. (2009) PIP(2)-binding site in Kir channels. Definition by multiscale biomolecular simulations. *Biochemistry* **48,** 10926–10933
18. Lin, C. W., Yan, F., Shimamura, S., Barg, S., and Shyng, S. L. (2005) Membrane phosphoinositides control insulin secretion through their effects on ATP-sensitive K^+ channel activity. *Diabetes* **54,** 2852–2858
19. Olsen, H. L., Hoy, M., Zhang, W., Bertorello, A. M., Bokvist, K., Capito, K., Efanov, A. M., Meister, B., Thams, P., Yang, S. N., Rorsman, P., Berggren, P. O., and Gromada, J. (2003) Phosphatidylinositol 4-kinase serves as a metabolic sensor and regulates priming of secretory granules in pancreatic beta cells. *Proc. Natl. Acad. Sci. U.S.A.* **100,** 5187–5192
20. Bai, J., Tucker, W. C., and Chapman, E. R. (2004) PIP_2 increases the speed of response of synaptotagmin and steers its membrane-penetration activity toward the plasma membrane. *Nat. Struct. Mol. Biol.* **11,** 36–44
21. Murray, D. H., and Tamm, L. K. (2011) Molecular mechanism of cholesterol- and polyphosphoinositide-mediated syntaxin clustering. *Biochemistry* **50,** 9014–9022
22. Murray, D. H., and Tamm, L. K. (2009) Clustering of syntaxin-1A in model membranes is modulated by phosphatidylinositol 4,5-bisphosphate and cholesterol. *Biochemistry* **48,** 4617–4625
23. Chung, S. H., Song, W. J., Kim, K., Bednarski, J. J., Chen, J., Prestwich, G. D., and Holz, R. W. (1998) The C2 domains of Rabphilin3A specifically bind phosphatidylinositol 4,5-bisphosphate containing vesicles in a Ca^{2+}-dependent manner. *In vitro* characteristics and possible significance. *J. Biol. Chem.* **273,** 10240–10248
24. Chen, Y. A., and Scheller, R. H. (2001) SNARE-mediated membrane fusion. *Nat. Rev. Mol. Cell Biol.* **2,** 98–106
25. Leung, Y. M., Kwan, E. P., Ng, B., Kang, Y., and Gaisano, H. Y. (2007) SNAREing voltage-gated K^+ and ATP-sensitive K^+ channels. Tuning beta-cell excitability with syntaxin-1A and other exocytotic proteins. *Endocr. Rev.* **28,** 653–663
26. Kang, Y. H., Leung, Y.-M., Manning-Fox, J., Xia, F., Xie, H., Sheu, L., Tsushima, R. G., Light, P., and Gaisano, H. Y. (2004) Syntaxin-1A inhibits cardiac KATP channels by its actions on nucleotide binding folds 1 and 2 of sulfonylurea receptor 2A. *J. Biol. Chem.* **279,** 47125–47131
27. Cui, N., Kang, Y., He, Y., Leung, Y. M., Xie, H., Pasyk, E. A., Gao, X., Sheu, L., Hansen, J. B., Wahl, P., Tsushima, R. G., and Gaisano, H. Y. (2004) H3 domain of syntaxin 1A inhibits KATP channels by its actions on the sulfonylurea receptor 1 nucleotide-binding folds-1 and -2. *J. Biol. Chem.* **279,** 53259–53265
28. Chang, N., Liang, T., Lin, X., Kang, Y., Xie, H., Feng, Z. P., and Gaisano, H. Y. (2011) Syntaxin-1A interacts with distinct domains within nucleotide-binding folds of sulfonylurea receptor 1 to inhibit β-cell ATP-sensitive potassium channels. *J. Biol. Chem.* **286,** 23308–23318
29. Lam, A. D., Tryoen-Toth, P., Tsai, B., Vitale, N., and Stuenkel, E. L. (2008) SNARE-catalyzed fusion events are regulated by Syntaxin1A-lipid interactions. *Mol. Biol. Cell* **19,** 485–497
30. Milosevic, I., Sørensen, J. B., Lang, T., Krauss, M., Nagy, G., Haucke, V., Jahn, R., and Neher, E. (2005) Plasmalemmal phosphatidylinositol-4,5-bisphosphate level regulates the releasable vesicle poolsize in chromaffin cells. *J. Neurosci.* **25,** 2557–2565
31. van den Bogaart, G., Meyenberg, K., Risselada, H. J., Amin, H., Willig, K. I.,

[5] T. Liang, L. Xie, C. Chao, Y. Kang, X. Lin, T. Qin, H. Xie, Z.-P. Feng, and H. Y. Gaisano, unpublished data.

Hubrich, B. E., Dier, M., Hell, S. W., Grubmüller, H., Diederichsen, U., and Jahn, R. (2011) Membrane protein sequestering by ionic protein-lipid interactions. *Nature* **479,** 552–555

32. Leung, Y. M., Kang, Y., Gao, X., Xia, F., Xie, H., Sheu, L., Tsuk, S., Lotan, I., Tsushima, R. G., and Gaisano, H. Y. (2003) Syntaxin 1A binds to the cytoplasmic C terminus of Kv2.1 to regulate channel gating and trafficking. *J. Biol. Chem.* **278,** 17532–17538
33. Chao, C., Liang, T., Kang, Y., Lin, X., Xie, H., Feng, Z. P., and Gaisano, H. Y. (2011) Syntaxin-1A inhibits KATP channels by interacting with specific conserved motifs within sulfonylurea receptor 2A. *J. Mol. Cell Cardiol.* **51,** 790–802
34. Pasyk, E. A., Kang, Y., Huang, X., Cui, N., Sheu, L., and Gaisano, H. Y. (2004) Syntaxin-1A binds the nucleotide-binding folds of sulphonylurea receptor 1 to regulate the K_{ATP} channel. *J. Biol. Chem.* **279,** 4234–4240
35. Lin, Y. W., Jia, T., Weinsoft, A. M., and Shyng, S. L. (2003) Stabilization of the activity of ATP-sensitive potassium channels by ion pairs formed between adjacent Kir6.2 subunits. *J. Gen. Physiol.* **122,** 225–237
36. Shyng, S. L., and Nichols, C. G. (1998) Membrane phospholipid control of nucleotide sensitivity of KATP channels. *Science* **282,** 1138–1141
37. James, D. J., Khodthong, C., Kowalchyk, J. A., and Martin, T. F. (2008) Phosphatidylinositol 4,5-bisphosphate regulates SNARE-dependent membrane fusion. *J. Cell Biol.* **182,** 355–366
38. McLaughlin, S., Wang, J., Gambhir, A., and Murray, D. (2002) PIP(2) and proteins. Interactions, organization, and information flow. *Annu. Rev. Biophys. Biomol. Struct.* **31,** 151–175
39. Ostenson, C. G., Gaisano, H., Sheu, L., Tibell, A., and Bartfai, T. (2006) Impaired gene and protein expression of exocytotic soluble *N*-ethylmaleimide attachment protein receptor complex proteins in pancreatic islets of type 2 diabetic patients. *Diabetes* **55,** 435–440